PACIFICHEM

2015 International Chemical Congress of Pacific Basin Societies

DECEMBER 15–20, 2015 • HONOLULU, HAWAII

www.pacifichem.org

Hyatt Regency Waikiki
Waioko Bllrm

Current Status and Future Prospect of Polymer Electrolyte Fuel Cells (#188)

Organized by: K. Miyatake, M. Tada, S. Sung, B. Pivovar, M. Hickner
Presiding: A. Herring, B. Pivovar

8:00 – 416. Development of perfluorinated alkaline membranes and advanced covalently tetherable cations. **B. Pivovar**, M. Sturgeon, H. Long
8:40 – 417. Anion exchange membranes composed of perfluoroalkyl and ammonium-functionalized oligophenylene main chains. **H. Ono***, J. Miyake, K. Miyatake
9:00 – 418. Polymer design of sterically-protected anion exchange membranes. **A.G. Wright**, S. Holdcroft*
9:20 – 419. Stabilization of anion exchange membranes to alkaline conditions for use in fuel cells. **J. Ward**, S. Holdcroft
9:40 Break
9:50 – 420. Next generation polymers for anion exchange membrane fuel cells. **A. Herring***, L. Matthew, D. Knauss, E. Coughlin, G. Voth, T. Witten
10:20 – 421. Structural modification on polystyrene based anion exchange membrane for optimizing membrane properties and performance. **S. Tuli**, R. Elgammal, T. Zawodzinski, T. Fujiwara*
10:40 – 422. Non-platinum catalysts for fuel cells obtained by sacrificial support method. **P. Atanassov***, K. Artyushkova, A. Serov, I. Matanovic, B. Kiefer, B. Halevi
11:10 – 423. Electrocatalysts for H2/Air(O2) anion exchange membrane fuel cells: Building a new non-pgm materials set. **A. Serov**, Y. Kim, M. Odgaard, B. Halevi, P. Atanassov

Hyatt Regency Waikiki
Waikiki Bllrm

Energy Storage in Chemical Bonds: Advances in Chemistry and Materials for Hydrogen Storage (#216)

Organized by: Z. Huang, P. Chen, T. Autrey, Q. Xu, C. Yoon, C. Jensen
Presiding: T. Autrey, C. Buckley

8:00 opening remarks
8:10 – 424. Materials-based hydrogen storage technologies: An overview from the U.S. DOE's perspective. **N.T. Stetson***
8:40 – 425. Heterolysis of molecular hydrogen for energy storage applications. **T. Autrey***
8:55 – 426. High temperature metal hydrides for concentrated solar thermal energy storage. **C. Buckley***, D. Sheppard, T. Humphries, M. Rowles, M. Sofianos, P. Javadian
9:15 – 427. Advances in the formation and regeneration of alane for hydrogen storage. **R. Zidan***, P.A. Ward, J.A. Teprovich , S. greenway, S. Mcwhorter
9:35 – 428. Amino alanes - possible new materials for hydrogen storage. **M. Felderhoff***
9:55 Break
10:05 – 429. Novel H, ,H interactions in chemical and metal hydrides. **S. McGrady**
10:25 – 430. Crystal structure analysis of Nb doped Ti-V-Cr hydrogen absorbing alloys using neutron diffraction. **E. Akiba***, S. Itano, H. Hirano, J. Matsuda, K. Ikeda, T. Otomo
10:45 – 431. Enhanced hydrogen generation performance of MgH_2 based hydrides. **L. Ouyang**, M. Zhu
11:05 – 432. Synthesis of metal@carbon hybrids and their enhanced effects on hydrogen storage properties of MgH_2. Y. Wang, **Y. Wang**, L. Jiao, H. Yuan
11:25 – 433. Redox reaction kinetics of metal oxides in chemical-looping processes for hydrogen production/storage systems using oxide ion conducting materials. **J. Otomo***, F. Kosaka, Y. Oshima, H. Hatano
11:40 – 434. Synthesis and energy device research of complex hydrides. **S. ORIMO***

Hawaii Convention Center
Halls I, II, III

New Generation of Electrochemical Energy Storage and Conversion System: Materials, Interface and In-situ Techniques (#250)

Organized by: Y. Yang, S. Meng, A. Yamada, Y. Sun

Poster Session
10:00 – 12:00

435. Graphene-based nanocomposites anode materials for lithium ion batteries. H. Kim, **K. Kim***
436. Toward high-volumetric energy density lithium-ion batteries: Particle density measurements of layered $LiCo_{1-x}Ni_xO_2$ with $0 \leq x \leq 1$. **K. Mukai***, H. Nakano
437. Effect of solid phase in fumed silic/lithium electrolyte solution dispersion system. **R. SOGAWA**, S. NAGATA, H. Maki, M. Mizuhata
438. Chemical reaction of organic carbonate on Li anode surface in Li-air battery based on tight-binding quantum chemical molecular dynamics. **K. Watanabe***, Y. Higuchi, N. Ozawa, M. Kubo
439. Exploration of Mn-based oxides micro/nanostructures as anode materials for advanced lithium ion batteries. X. Gu, N. Wang, **J. Yang**, Y. Qian
440. Synthesis and characterization of ordered mesoporous electrode materials for lithium storage. S. Park, K. Kim, H. Lee, G. Park, **J. Kim***
441. Novel lithium ion conducting oxides based on $LiScO_2$. **G. Zhao**, I. Muhammad, K. Suzuki, M. Hirayama, R. Kanno*
442. Effects of sulfur electrolyte additives on solid electrolyte interfaces of lithium-ion batteries. **S. Kikuzaki**, C. Yogi, T. Sanada, K. Kojima, M. Katayama, Y. Inada, T. Ohta
443. $Li_3V_xMn_{1-x}(PO_4)_3$ as a positive electrode material for high rate rechargeable lithium batteries. **J. Park**, S. Myung
444. All solid state batteries using epitaxial-film cathode with a lithium-rich layered rocksalt structure. **M. Hirayama***, Y. Zheng, K. Suzuki, R. Kanno
445. Effects of K-ion doping on electrochemical performance of $Na_3V_2(PO_4)_3$ cathode materials for Na-ion batteries. **J. Eom***
446. Co-precipitation synthesis of low carbon-coated $LiMn_{0.6}V_{0.4}PO_4$ as high-rate cathode materials for lithium ion battery. W. Ma, H. Chen, C. Chang, **Y. Chen-Yang***
447. Synthesis and electrochemical characteristics of nano porous silicon/carbon composite anode for lithium ion battery. **J. Lee***, H. Lee, J. Park
448. Eye-inspired radical scavenger: Polydopamine as an electrolyte additive for improved cycle performance of Li-air batteries. **S. Kim**, J. Choi*, H. Lee*
449. Lithium ion conductor with Argyrodite type structure in the Li-Ge-P-S system. **Y. Inoue**, K. Suzuki, M. Hirayama, R. Kanno
450. Intercalation of sodium and magnesium into boron/carbon materials. **H. Higuchi***, M. Kawaguchi
451. Green, large-scale synthesis of hierarchical nanorod assembly of polyaniline for supercapacitor applications. **D. S***
452. Nickel–manganese oxide on MWCNTs/CFP substrate as supercapacitor electrode. X. Zhang, H. Wang, Y. Huang, **Q. Li***
453. Unique nano-architecture electrodes for high-performance supercapacitor. **G.G. Khan***, A.K. Singh , D. Sarkar
454. Reaction and transport of alkalimetal ion on SnO_2 thin film fabricated by liquid phase deposition method. **Y. SHIBATA**, H. Maki, M. Mizuhata
455. Electrocatalytic oxygen evolution by polyanion-based manganese compounds. **T. Takashima***, H. Irie
456. Efficient electrocatalytic electrodes for energy storage devices based on conducting polymers. **P. Talemi***
457. High-energy-density proton redox capacitor using quinonic compounds couple. **T. Tomai***, D. Komatsu, I. Honma
458. Reversible oxidation of Pt nanoparticles: In situ hard X-ray photoelectron spectroscopy studies under H_2O and MeOH atmospheres. **H. Wang**, Y. Takagi, Y. Uemura, O. Sekizawa, T. Uruga, M. Tada, Y. Iwasawa*, **T. Yokoyama***, H. Yoshikawa
459. High contrast and complementary electrochromic device based on a WO_3 film and an organic solution with broadly absorbing from the visible and the infrared. **D. Weng***, M. Li, J. Zheng, C. Xu*
460. Charge/discharge behavior of Co-doped Li_2O of a battery utilizing a redox of oxide and peroxide. **H. Kobayashi***, M. Hibino, Y. Ogasawara, T. Kudo, S. Okuoka, H. Ono, K. Yonehara, Y. Sumida, N. Mizuno
461. Far-red sensitive squaraine dyes with extended π-conjugation toward anchoring group for molecular photovoltaics. G.M. Shivashimpi, N. Fujikawa, G. Kapil, Y. Ogomi, **S.S. PANDEY***, Y. Yamaguchi, S. Hayase
462. Fabrication of graphene/Poly(styrene-sulfonic acid-*g*-aniline) composites for high performance supercapacitor electrodes. **j. lee**, j. jo, k. Kim, W. Jo*
463. Co_3O_4 supercrystals with enhanced performances in energy storage. Y. Gong, S. Lu, H. Chen, C. Wang, **F. Li**
464. Molecular design and photophysical characterization of squaraine dyes with varying fluoroalkyl substituents. **T. Morimoto***, N. Fujikawa, Y. Ogomi, Y. Yamaguchi, S.S. PANDEY, T. Ma, S. Hayase
465. Energy storage by proton-coupled electron transfer reactions of Ru complexes. **D. MOTOYAMA**, H. Ozawa, M. Haga*
466. Investigating small-polarons in Mo/W-$BiVO_4$: Large implications for solar H_2 production. **V. Jovic***, J. Laverock, A.J. Rettie, J. Zhou, C.B. Mullins, D. Wilson, T. Söhnel, K.E. Smith
467. Porous graphene structure from electrochemical exfoliation for supercapacitor applications. **S. Jung**, H. Jung, J. Kong
468. Performance enhancement of planar heterojunction perovskite solar cells by *n*-doping of electron transporting layer. **S. Kim**, S. Bae, W. Jo*
469. Membrane-free wastewater electrolysis cell for decentralized molecular hydrogen production: Current and energy efficiency. **K. Cho***, M. Hoffmann
470. Surface enhanced IR absorption spectro-electrochemistry of immobilized [NiFe] hydrogenase on graphene oxide/Au hybrid electrodes. **H. Gatemala***, L.C. Perez, T. Harris, S. Frielingsdorf, O. Lenz, C. Thammacharoen, S. Ekgasit, I.M. Weidinger, A. Fischer, N. Heidary*, K.H. Ly*, I. Zebger*
471. Creation of chiral ionic plastic crystals and its proton conductivity. **T. Yamada***, M. Matsuki, N. Kimizuka
472. Interrelation between processing condition, morphology, crystal orientation, and efficiency of $CH_3NH_3PbI_3$-based perovskite solar cells. **S. Bae**, S. Han, T. Shin, W. Jo*

Hyatt Regency Waikiki
Kou Ballrm

Artificial Photosynthesis: Bio-inspired Chemistry for Solar Fuel Production (#278)

Organized by: H. Hashimoto, Y. Amao, J. Zhang, T. Moore, B. Koivisto
Presiding: Y. Amao, H. Hashimoto, B.D. Koivisto, T.A. Moore, J. Zhang

8:00 – 473. Mechanism of light-induced water splitting – learning from nature's ingenious concept. **W. Lubitz***
8:30 – 474. Molecular photosynthesis: Such stuff as dreams are made on. **M. Bonchio***
8:45 – 475. In-situ passivation layer protected Si photoanode with sparse catalysts for stable and quantitative solar water oxidation. **K. Sun**, W.G. Hale, B.S. Brunschwig, N.S. Lewis
9:00 – 476. Birnessite as structural motif for the development of oxygen evolution reaction (OER) electrocatalysts. **J.H. Baricuatro***, F.H. Saadi, A. Carim, J.M. Velázquez, M.P. Soriaga
9:15 – 477. Bioinspired catalytic systems and technological applications of hydrogen. **V. Artero***
9:45 – 478. Proton-coupled electron transfer processes in artificial photosynthesis. **L. Hammarström***, S. Glover, G. Parada, T. Markle, M. Bourrez, p. Dongare, S. Ott
10:00 – 479. Evaluation of oxidation ability for plasmon-induced charge separation: Approach from coordinative dissolution and surface passivation of gold nanoparticles. **H. Nishi***, T. Tatsuma*
10:15 – 480. Bio-nano photocatalytic systems for solar hydrogen production. **E. Rozhkova***, P. Wang
10:30 – 481. Photocatalytic hydrogen production using carbon nitrides with enzymatic and synthetic biomimetic co-catalysts. **C.A. Caputo**, M.A. Gross, E. Reisner
10:45 – 482. Novel metal-peptide conjugates for CO_2 reduction catalysts. **H. Ishida***
11:15 – 483. BODIPY as a non-innocent π-spacer in organic dye motifs: Toward next-generation photovoltaic applications. **B.D. Koivisto***
11:30 – 484. Achieving enzyme-like behavior with amino acids and peptides in the outer coordination sphere of hydrogenase mimics. **W. Shaw***, A. Dutta, J. Roberts, A. Jain, M. Reback
11:45 – 485. Artificial light-driven proton pumps as mimics for natural photosynthesis. C.D. Sanborn, R. Reiter, W. White, **S. Ardo**

Hyatt Regency Waikiki
Mauka Bllrm

Homogeneous Catalysis Methodologies for the Upgrading of Biomass Derived Molecules (#301)

Organized by: J. Gordon, R. Baker, T. Ikariya
Presiding: T. Ikariya

8:00 – 486. Strategies for biofeedstock processing via tandem catalytic C-O hydrogenolysis. **T.J. Marks**
8:35 – 487. Catalytic conversion of renewable resources into bulk and fine chemicals. **J.G. de Vries***
9:10 break
9:20 – 488. Commercialization of olefin metathesis for use in the world's first biorefinery plants. **R.L. Pederson***
9:45 – 489. Hydrogenation and dehydrogenation processes based on bifunctional Ru and Ir complexes bearing protic amine chelate ligands. **Y. Kayaki***
10:10 – 490. Hydrogen management for transformation of CO_2- and biomass-derived feedstock using molecular surface. **S. SAITO***
10:35 break
10:45 – 491. High efficient tetradentate ruthenium catalyst for esters reduction. **X. Zhang**

*** Principle Author**

Photographing of presentations and/or taping of talks is prohibited unless permission is obtained from the symposia organizers and individual presenters. Final Pacifichem 2015 program online at: http://pacifichem.org/onlineprogram

Performance Enhancement of Planar Heterojunction Perovskite Solar Cells by *n*-Doping of Electron Transporting Layer

Shin Sung Kim, Seunghwan Bae and Won Ho Jo*

Advanced Materials for Organic Photovoltaic Lab.
Department of Materials Science & Engineering, Seoul National University

GRL Global Research Laboratory
서울대 + Univ. of Massachusetts
Nanomaterials for Environmentally Friendly Energy Conversion

Introduction

❖ Why Perovskite Solar Cells?

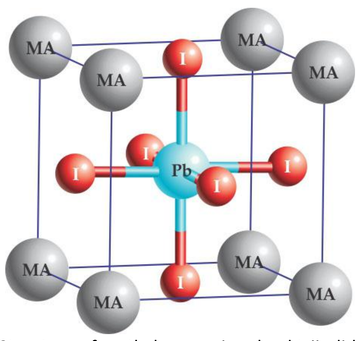

Structure of methylammonium lead triiodide (MAI, $CH_3NH_3PbI_3$)

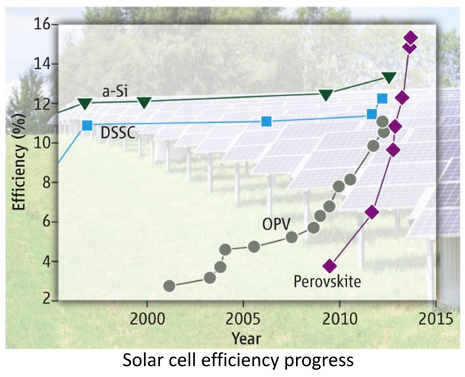

Solar cell efficiency progress

▪ **Large absorption coefficient**

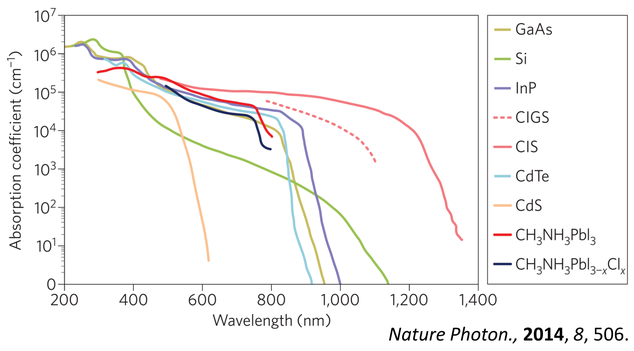

Nature Photon., **2014**, *8*, 506.

▪ **Easy and low-cost process**

▪ **High charge carrier mobility**

▪ **Easily tunable optoelectronic properties**

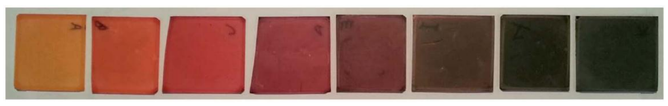

Energy Environ. Sci., **2014**, *7*, 982.

▪ **Extremely large exciton diffusion length**

Perovskite	Species	D (cm^2 s^{-1})	L_D (nm)
$CH_3NH_3PbI_{3-x}Cl_x$	Electrons	0.042 ± 0.016	1069 ± 204
	Holes	0.054 ± 0.022	1213 ± 243
$CH_3NH_3PbI_3$	Electrons	0.017 ± 0.011	129 ± 41
	Holes	0.011 ± 0.007	105 ± 32

Science, **2013**, *342*, 341.

❖ Effect of *n*-Doping to Fullerene Derivatives

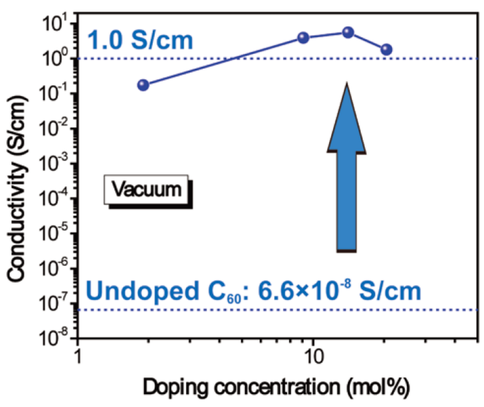

J. Am. Chem. Soc., **2012**, *134*, 3999.

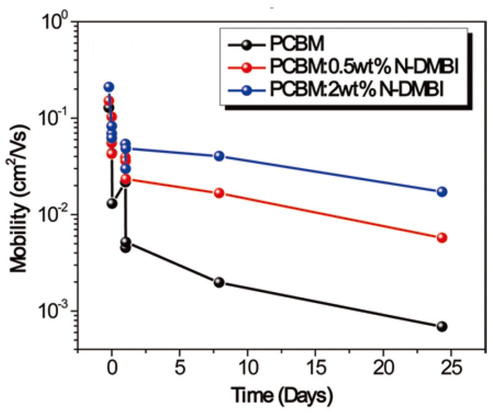

J. Am. Chem. Soc., **2010**, *132*, 8852.

✓ **Electric conductivity and electron mobility of fullerene derivatives were significantly enhanced by *n*-doping.**

Objectives

➢ **To increase the electric conductivity of PCBM by *n*-doping**

➢ **To enhance the photovoltaic performance of planar heterojunction perovskite solar cells by *n*-doping to the electron transporting layer (ETL)**

➢ **To examine the effect of doping according to the PCBM layer thickness**

Results

❖ Synthesis of Dopant and Characterization of Doping

▪ **Synthesis of DMBI**

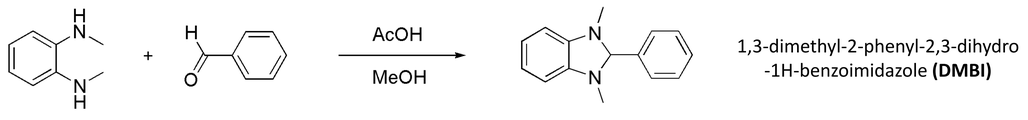

1,3-dimethyl-2-phenyl-2,3-dihydro-1H-benzoimidazole **(DMBI)**

▪ **^{1}H NMR**

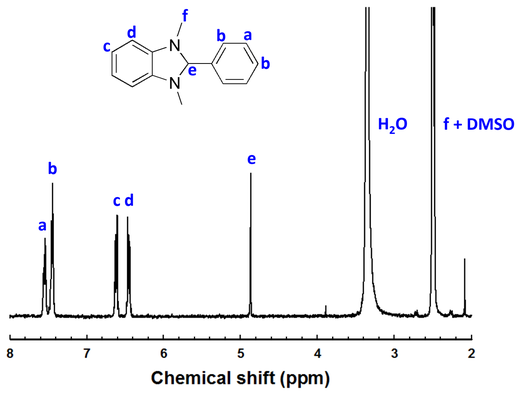

▪ **Absorption spectra**

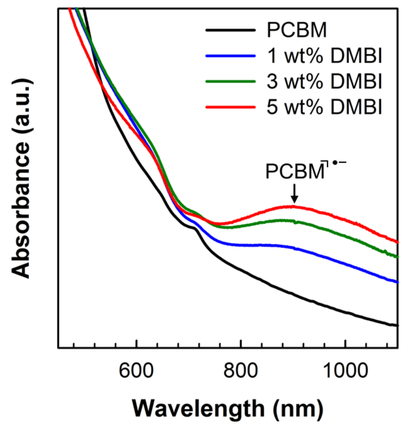

▪ **UPS spectra**

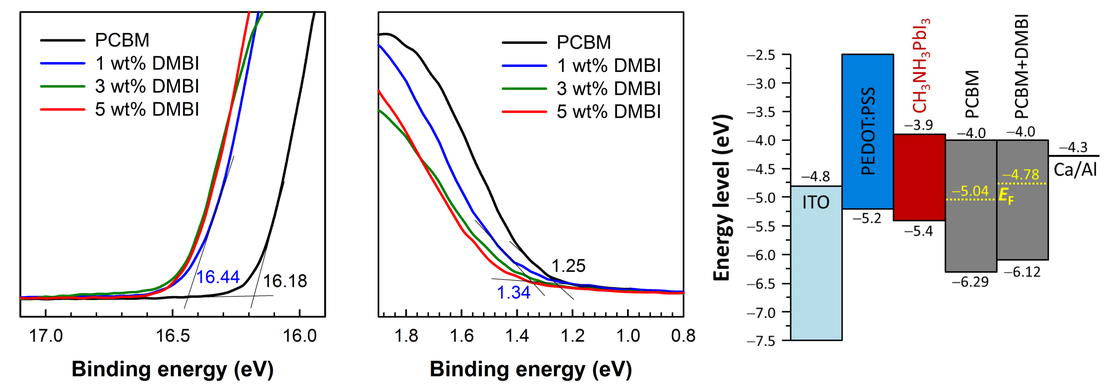

❖ Photovoltaic Performance of Device with *n*-Doped PCBM

▪ **Device fabrication**

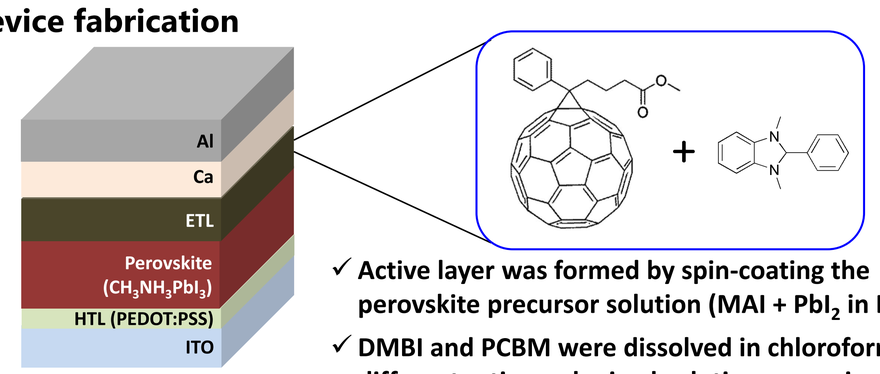

✓ **Active layer was formed by spin-coating the perovskite precursor solution (MAI + PbI_2 in DMSO).**

✓ **DMBI and PCBM were dissolved in chloroform for different ratio, and mixed solution was spin-coated to form the *n*-doped ETL.**

▪ **Thin layer of PCBM**

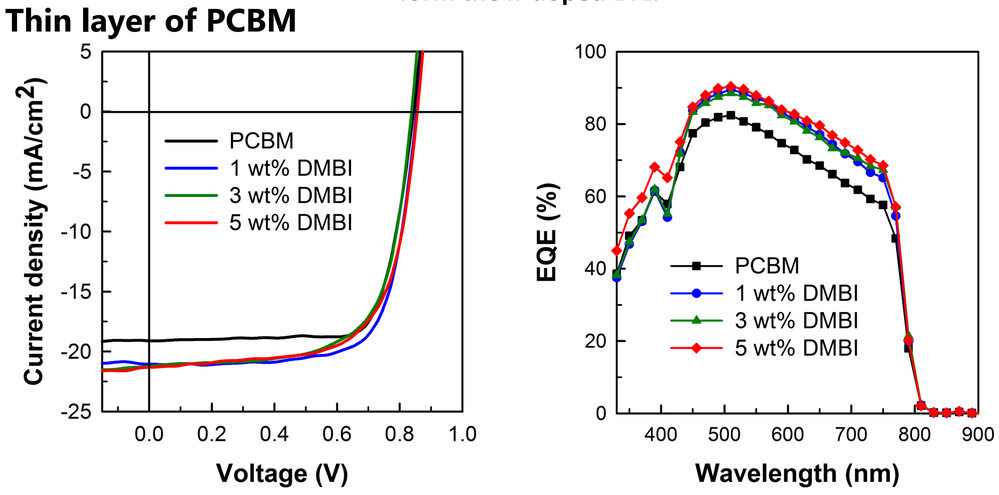

▪ **Thick layer of PCBM**

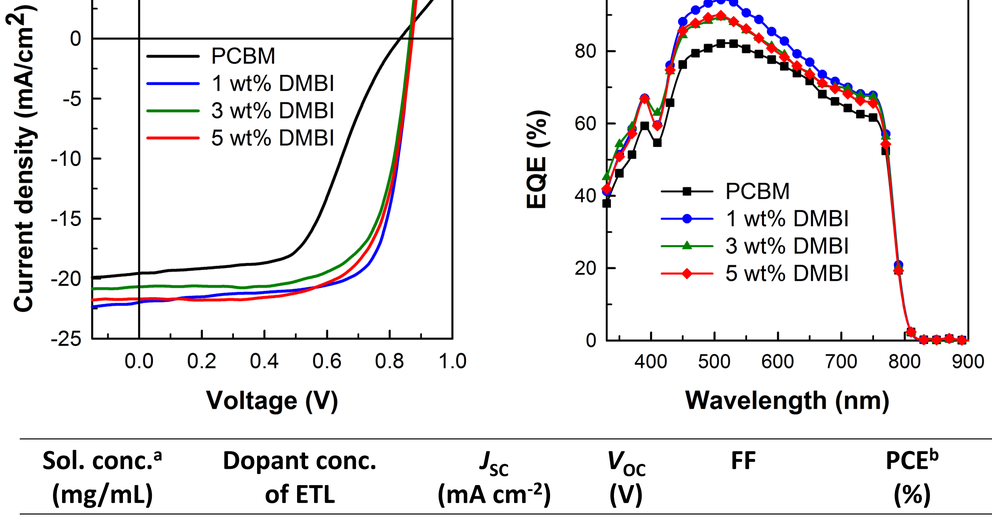

Sol. conc.[a] (mg/mL)	Dopant conc. of ETL	J_{SC} (mA cm^{-2})	V_{OC} (V)	FF	PCE[b] (%)
10	Pure PCBM	19.1	0.84	0.77	12.3 (11.0)
10	1 wt% DMBI	21.0	0.85	0.73	13.0 (12.1)
10	3 wt% DMBI	21.2	0.84	0.68	12.1 (11.1)
10	5 wt% DMBI	21.3	0.86	0.67	12.3 (11.1)
20	Pure PCBM	19.6	0.83	0.55	8.9 (7.9)
20	1 wt% DMBI	22.0	0.87	0.72	13.8 (12.2)
20	3 wt% DMBI	20.7	0.86	0.70	12.4 (11.2)
20	5 wt% DMBI	21.7	0.87	0.69	13.0 (11.6)

[a]10 and 20 mg/mL chloroform solutions are used for fabrication of 50 and 105 nm thick ETL, respectively.
[b]Average PCE values based on at least 10 devices are indicated in parentheses.

Conclusions

➢ **Addition of DMBI raises the Fermi level of PCBM toward the LUMO energy level, indicative of *n*-doping.**

➢ **The solar cell device with *n*-doped PCBM as electron transporting layer has shown a high PCE of 13.8% with 10% enhanced J_{SC} of 22.0 mA/cm^2.**

➢ ***n*-Doping enhances the electric conductivity of PCBM, then facilitate the increase of PCBM layer thickness.**

Performance enhancement of planar heterojunction perovskite solar cells by *n*-doping of electron transporting layer

Shin Sung Kim, Seunghwan Bae, Won Ho Jo†

Department of Materials Science and Engineering, Seoul National University

Recently, organic-inorganic hybrid perovskite has attracted great attention as a next generation material for solar cell because of its superior intrinsic properties such as extremely long exciton diffusion length, high absorption coefficient, and excellent carrier transport. Most of state-of-the-art perovskite solar cells utilize TiO_2 and 2,2',7,7'-tetrakis(*N*,*N*-bis(*p*-methoxy-phenyl)amino)-9,9'-spirobifluorene as electron and hole transporting materials, respectively. However, since the formation of mesoporous TiO_2 layer requires high temperature sintering process, all solution-processible bilayer structure has been investigated as an alternative device structure by several groups. This planar heterojunction structure utilizes commonly PCBM and PEDOT:PSS as electron and hole transporting materials, respectively. In this architecture, sufficiently thick PCBM layer is required to prevent direct contact between perovskite film and metal electrode. However, relatively low electron mobility and low electric conductivity of PCBM may provide a limit to achieve high power conversion efficiency (PCE) of the device with thick PCBM layer. In this study, an *n*-type dopant, 1,3-dimethyl-2-phenyl-2,3-dihydro-1H-benzoimidazole (DMBI), was added into PCBM layer to enhance the electric conductivity of PCBM. Addition of a small amount of DMBI raises the Fermi level of PCBM toward the LUMO energy level, indicative of *n*-doping and an increase of free electrons. As a result, the solar cell device with *n*-doped PCBM as electron transporting layer shows a remarkable enhancement of short-circuit current density (J_{SC}) and the PCE. While the device without the dopant exhibits S-shaped curve with a fill factor (FF) of 0.55, the device with 1% doped PCBM shows higher FF of 0.72. Consequently, the doped deice have shown a high PCE of 13.8% with 10% enhanced J_{SC} of 22.0 mA/cm^2. Particularly, the effect of doping was more prominent when the thickness of PCBM layer was increased.